



**Metal Oxide Containing Mesoporous Silica with Bicontinuous “Plumber’s Nightmare” Morphology from a Block Copolymer–Hybrid Mesophase\*\***

Adam C. Finnefrock, Ralph Ulrich, Alexander Du Chesne, Christian C. Honeker, Kai Schumacher, Klaus K. Unger, Sol M. Gruner, and Ulrich Wiesner\*

The synthesis of mesoporous materials by using organic molecules as structure-directing agents or templates is an area of rapid growth with diverse applications, such as separation technology and catalysis. Block copolymers can be regarded as macromolecular analogues of low molecular weight surfactants.<sup>[1]</sup> Use of block copolymers was recently shown to extend the pore sizes of ordered porous silica to hundreds of Ångströms.<sup>[2–5]</sup> Combined principles of polymer, colloidal, and inorganic chemistries were used to synthesize materials with uniform and adjustable pore sizes and with thick, hydrothermally stable walls.<sup>[6]</sup> Both two-dimensional hexagonal structures and three-dimensional cubic morphologies with more accessible pores have been synthesized. The synthetic strategy has been generalized for various metal oxides and hierarchical oxide structures.<sup>[7–9]</sup>

Recently, we showed that unprecedented morphology control is obtained for nanostructured materials by changing from conventional silicon precursors to organically modified ceramic (ormocer) precursors in the block copolymer directed synthesis.<sup>[4]</sup> Most of the mesophase morphologies observed in block copolymers or copolymer–homopolymer mixtures have been obtained for such organic–inorganic hybrid materials.<sup>[10]</sup> The basis for this morphological control is a unique polymer–ceramic interface which can be characterized by solid-state NMR techniques.<sup>[11]</sup> The hydrophilic blocks of the amphiphilic copolymers are completely integrated into the ceramic phase. This leads to a “quasi-two-phase system” that allows for a more rational design of hybrid morphology based on the current understanding of the phase behavior of block copolymers and copolymer–homopolymer mixtures.<sup>[12]</sup>

Here we describe the block copolymer directed preparation, characterization, and properties of metal oxide containing mesoporous silica in an area of the block copolymer phase space where a double Gyroid phase might be expected.<sup>[12]</sup> Ordered bicontinuous nanoporous and nanorelief materials with the Gyroid morphology have been realized in ultrathin films.<sup>[13]</sup> The synthesis of such structures in the bulk is still a challenge. To our surprise the data presented below on the bulk materials, both before and after calcination, are consistent with a “Plumber’s Nightmare”<sup>[14]</sup> morphology. This refers to subtle, poorly understood differences of phase behavior between the present hybrid materials and block copolymer–homopolymer mixtures. Because of its interwoven and regular, branched cubic bulk structure, the resulting mesoporous material is expected to provide excellent mass-transfer kinetics in catalytic and separation technologies. The approach based on ormocer–block copolymer combinations may therefore significantly expand the property profile of mesoporous materials.

An amphiphilic diblock copolymer, namely, poly(isoprene-*b*-ethylene oxide) (PI-*b*-PEO), with a total number average molecular weight of 16.4 kg mol<sup>-1</sup> and a volume fraction of PEO of 35% was used as the structure-directing agent. Anionic polymerization was employed to obtain this polymer with a narrow molecular weight distribution (polydispersity < 1.1).<sup>[15]</sup> The pure diblock copolymer exhibits a melt morphology of hexagonally packed PEO cylinders in a PI matrix, as expected for such a volume fraction.<sup>[12]</sup> Mixing of the ormocer precursors (3-glycidyloxypropyl)trimethoxysilane (GLYMO) and aluminum *sec*-butoxide with the diblock copolymer in a molar ratio of 80:20 was performed by using a recently described procedure.<sup>[10]</sup>



The volume fraction of the PI phase of the as-made material was calculated to be 0.36. It is assumed that there is no phase mixing between the PI (density 0.91 g cm<sup>-3</sup>) and the inorganic/PEO phase (density 1.4 g cm<sup>-3</sup>).<sup>[10]</sup> The organic–inorganic nanocomposite was then calcined to obtain a mesoporous material. Calcination was achieved by heating in several stages up to 600 °C in air with an overall heating rate of approximately 1 K min<sup>-1</sup>. Elemental analysis after calcination indicated 0.1 wt% C and 1.5 wt% H. The weight loss, measured by thermogravimetric analysis (TGA) as 75%, compared well with the theoretical prediction of 78%.

Bright-field transmission electron microscopy (TEM) data on as-made and calcined materials are shown in Figure 1. Bright areas correspond to the minor phase that either consists of PI (uncalcined) or voids (calcined), while dark areas correspond to the major PEO-rich ceramic phase. For both samples the classic cubic fourfold and threefold orientations are shown. In particular, in the case of the calcined material it is easy to identify thin, connected volumes (channels) with fourfold and threefold (“wagonwheel”)

[\*] Prof. Dr. U. Wiesner  
Department of Materials Science and Engineering  
Cornell University  
329 Bard Hall, Ithaca, NY 14853 (USA)  
Fax: (+1) 607-255-2365  
E-mail: ubw1@cornell.edu

Dr. R. Ulrich, Dr. A. Du Chesne, Dr. C. C. Honeker  
Max-Planck-Institut für Polymerforschung  
Ackermannweg 10, 55128 Mainz (Germany)

Dr. A. C. Finnefrock, Prof. Dr. S. M. Gruner  
Physics Department, Cornell University  
Clark Hall, Ithaca, NY 14853-2501 (USA)

Dr. K. Schumacher, Prof. Dr. K. K. Unger  
Institut für Anorganische und Analytische Chemie  
Johannes-Gutenberg-Universität  
Duesbergweg 10–14, 55099 Mainz (Germany)

[\*\*] This work was supported by the National Science Foundation (DMR-0072009), the Cornell Center for Materials Research (NSF DMR-9632275), and the Department of Energy (DE-FG02-97ER62443). We also acknowledge very helpful discussions with G. E. S. Toombes.

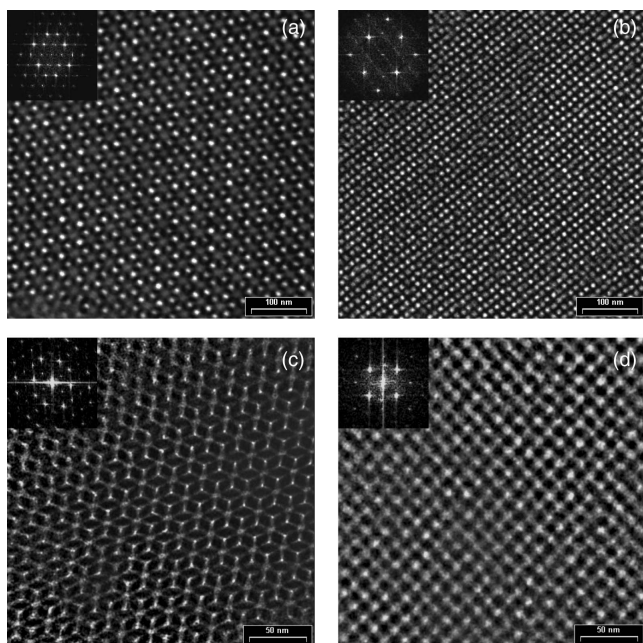


Figure 1. Bright-field TEM images from as-made (top) and calcined material (bottom) highlighting the threefold (a, c) and fourfold (b, d) projections of the cubic phase. The images from calcined material exhibit even greater contrast due to the removal of all organic moieties. This allows for the convenient identification of the bicontinuous nature of the structure. Insets in each panel show the computed Fourier diffraction patterns. These materials show a striking degree of order over broad regions.

orientations, typical of a bicontinuous cubic structure. Furthermore, as demonstrated by scanning electron microscopy (SEM), the materials show a remarkably large average grain size (data not shown). It was not uncommon to find grains spanning the entire area of a grid mesh (approximately 100  $\mu\text{m}$  in diameter). The beautiful micrographs therefore suggest the existence of a highly ordered bicontinuous cubic mesostructure.

We performed small-angle X-ray scattering (SAXS) experiments on both as-made and calcined samples to identify the underlying symmetry and further elucidate the long-range structure (Figure 2). The X-ray patterns indicate a high degree of ordering, out to  $q^2 = h^2 + k^2 + l^2 = 50$  and  $q^2 = 32$  reciprocal lattice units for the as-made and calcined samples, respectively. This is remarkable, given that the structure is highly disordered on length scales of a few Ångströms. Consistent with the large grain sizes observed by electron microscopy, the distinct peaks in the images imply that the X-ray beam ( $< 0.1 \text{ mm}^2$ ) averages

only over a limited number of crystallites with different orientations. Beneath each SAXS image in Figure 2 is a plot of the peak positions. By using systematic algorithms,<sup>[16]</sup> a structure was solved for each set of peaks that could originate from a single microdomain within the scattering volume. The peaks are colored according to the microdomain; peaks are visible from five microdomains within the uncalcined image, and from six microdomains within the calcined image.

It is usually difficult to determine the lattice symmetries of classic powder diffraction patterns consisting of a limited number of concentric rings. The inclusion of azimuthal information, such as is present in Figures 2a and 2b, places strong constraints on the possible symmetry groups and unit cell lengths of the sample. The reciprocal-space SAXS data is consistent with  $Im\bar{3}m$  symmetry, and the lattice basis lengths were determined to be 630 and 395 Å for the as-made and calcined samples, respectively, consistent with the analysis of the TEM data.

Figure 3 contrasts two structures derived from infinite periodic minimal surfaces, namely, the Plumber's Nightmare and the Gyroid. The TEM data strongly suggest a bicontinuous cubic morphology. The TEM data, together with the X-ray  $Im\bar{3}m$  symmetry, suggest a Plumber's Nightmare-like phase,<sup>[14]</sup> and exclude the Gyroid and Double Diamond.<sup>[12]</sup> A detailed description of the X-ray analysis will be presented

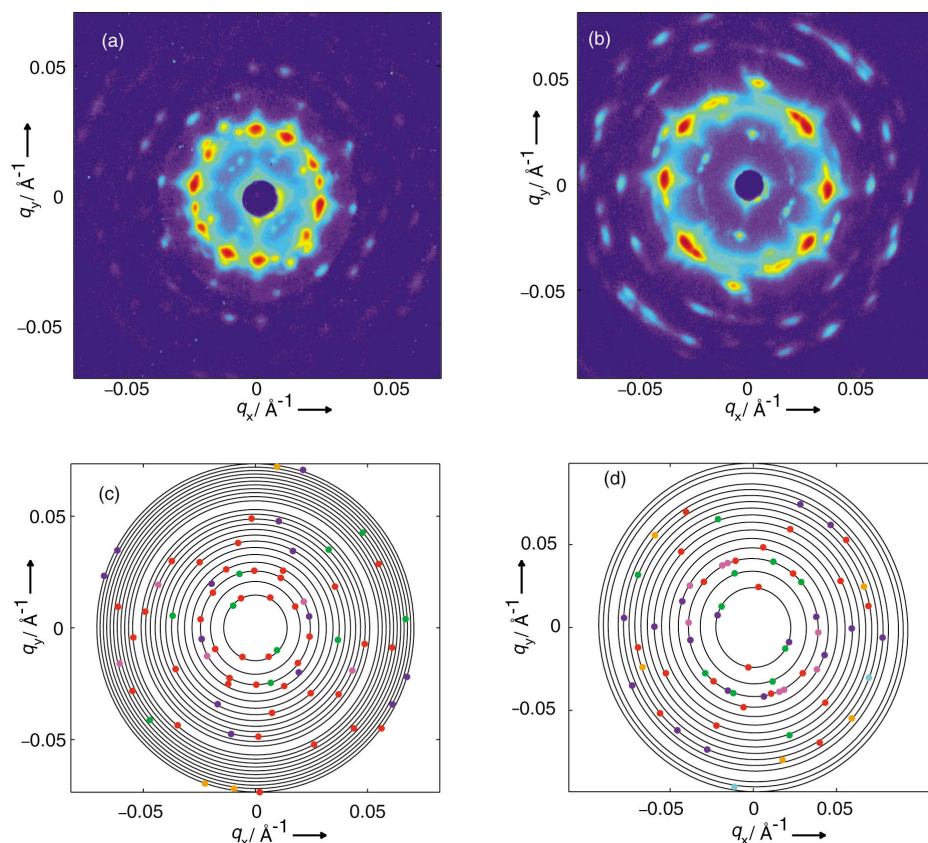


Figure 2. SAXS images (top) obtained from as-made (a) and calcined (b) samples. The false-color scale (ascending from blue to red) corresponds to logarithmic X-ray intensity. Indexed peak positions (bottom) for as-made (c) and calcined (d) samples. Peaks from the same crystallite are colored identically. All of these peaks can be assigned to five microdomains within the scattering volume for the as-made (c), and six microdomains for the calcined sample (d). The radii of the circles are given by  $q = \sqrt{h^2 + k^2 + l^2}$ , where  $h, k, l$  are integers allowed by the  $Im\bar{3}m$  symmetry group. The apparent gap results because  $q^2 = 28$  units is not the sum of any three squares of integers.

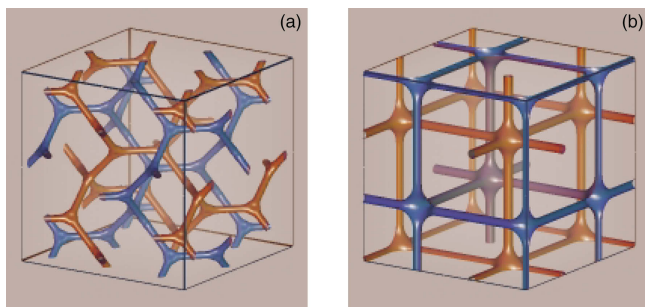


Figure 3. Real-space image of a stick structure derived from the Plumber's Nightmare (a). For comparison, the real-space image of a Gyroid-derived structure is shown (b). The graphics were generated by using the following website: <http://msri.org/publications/sgp/SGP/>. Blue and brown colors serve to distinguish the two distinct three-dimensional channel systems.

elsewhere.<sup>[16]</sup> A powder-diffraction pattern of a block copolymer derived mesoporous silicate, with a very different structure formation process, was also reported to be consistent with  $Im\bar{3}m$  symmetry.<sup>[6]</sup> However, in that case the limited number of diffracted orders necessarily meant that the symmetry assignment was more tentative.

It is striking that the symmetry is so well-preserved after calcination, even though the lattice constant falls to approximately 60% of the value for the uncalcined material (the cell volume drops to about 25%). This indicates that the bonding network formed by the inorganic precursors is extremely robust. This may be a general feature of the block copolymer derived ormocer materials. After calcination the bulk material consists of an aluminosilicate matrix interwoven with two discrete, continuous nanochannel systems that do not touch each other (see Figure 3) and result in a mesoporous material with open and accessible pores. Indeed, it exhibits a nitrogen sorption isotherm of type IV according to BDDT classification, with a specific surface area of  $300 \text{ m}^2 \text{ g}^{-1}$  according to the Brunauer–Emmett–Teller (BET) method (data not shown).<sup>[17]</sup> Calculation of the pore size distribution from the desorption branch of the isotherm reveals a slightly bimodal pore size distribution with an average pore diameter according to Barrett–Joyner–Halenda (BJH) of 8.9 nm.<sup>[18]</sup> The specific pore volume can be calculated by the Gurvitch rule to be  $0.47 \text{ mL g}^{-1}$ .<sup>[19]</sup> From earlier NMR studies, we know that about half of the aluminum is incorporated in the silicon network as fourfold-coordinated aluminum. Calcination of the as-made material leads to an increase in the amount of such in-frame aluminum with respect to the precursor material and thus provides a pathway to materials with acid catalytic activity.

In summary, we have described the synthesis and characterization of a metal oxide containing mesoporous silica from a block copolymer–hybrid mesophase. Using a combination of SAXS and TEM we have shown that the structure of the mesophase is most consistent with the  $Im\bar{3}m$  cubic space group associated with the bicontinuous Plumber's Nightmare morphology. The structure exhibits unusually large grain sizes (10–100  $\mu\text{m}$ ) and is preserved after calcination. Nitrogen sorption isotherms clearly demonstrate the accessibility of the resulting interwoven networks of channels. Finally we have demonstrated that by this synthetic method, metal oxides

imperative for catalytic applications<sup>[20]</sup> (e.g., alumina, titania) can be incorporated conveniently. In analogy with monomer–surfactant–water systems, we expect to find a variety of bicontinuous cubic phases as the stoichiometric ratios of PI, PEO, and inorganic components are altered.<sup>[21]</sup> This may elucidate the origin for the occurrence of the present Plumber's Nightmare symmetry rather than the Gyroid symmetry. Studies along these lines are now underway.

### Experimental Section

Adsorption and desorption isotherms were measured at 77 K on a Quantachrome Autosorb 6B (Quantachrome Corporation, Boynton Beach, FL). The samples were outgassed at 423 K and 1 mPa for 13 h before measurements were made.

TEM: The organic–inorganic hybrid sample was used as synthesized. The calcined sample was manually powdered and embedded in UHU glue (Henkel). Ultrathin sections (thickness 50–100 nm) were produced with a Leica-ultramicrotome (UCT) at  $-55^\circ\text{C}$ . Sections were floated off the diamond knife onto aqueous DMSO solution, transferred to grids, and investigated unstained. TEM was performed on a Leo 912  $\Omega$  (tungsten filament) operated at 120 kV with an objective aperture angle of 16.5 mrad. All images were taken in the elastically filtered imaging mode. Contrast of the unstained, uncalcined samples was very weak, but the morphology of the samples could be clearly observed at a defocus of about 2.5  $\mu\text{m}$ . The organic–inorganic (aluminosilicate) hybrid appears as the dark phase. Images were recorded with a slow-scan CCD camera (lateral resolution  $1000 \times 1000$  pixels, 14-bit gray values), and fast Fourier transforms were calculated by means of an SIS-AnalySIS<sup>®</sup> image-processing system.

SAXS:  $\text{Cu}_{K\alpha}$  X-rays ( $\lambda = 1.54 \text{ \AA}$ ) were generated on a Rigaku RU300 rotating-anode generator, focused by Franks mirror optics, and then imaged with a home-built  $1000 \times 1000$  CCD detector (as in ref. [22]). The data of the uncalcined sample were recorded with 42 exposures over 9.3 h, to maximize the signal-to-noise ratio and dynamic range. The calcined sample only required 12 exposures totaling 18 min. The  $q$ -dimensions of each image were calibrated with silver behenate ( $d = 58.376 \text{ \AA}$ ) and silica sphere ( $R = 278 \text{ \AA}$ ) references. (The reader is referred to ref. [16] for more details of the SAXS data treatment and analysis.)

Received: October 2, 2000 [Z15898]

- [1] B. M. Discher, Y. Y. Won, D. S. Ege, J. C. M. Lee, F. S. Bates, D. E. Discher, D. A. Hammer, *Science* **1999**, *284*, 1143.
- [2] S. A. Bagshaw, E. Prouzet, T. J. Pinnavaia, *Science* **1995**, *269*, 1242.
- [3] C. G. Göltner, M. Antonietti, *Adv. Mater.* **1997**, *9*, 431; C. G. Göltner, S. Henke, M. C. Weissenberger, M. Antonietti, *Angew. Chem.* **1998**, *110*, 633–636; *Angew. Chem. Int. Ed.* **1998**, *37*, 613.
- [4] M. Templin, A. Franck, A. Du Chesne, H. Leist, Y. Zhang, R. Ulrich, V. Schädler, U. Wiesner, *Science* **1997**, *278*, 1795.
- [5] D. Zhao, J. Feng, Q. Huo, N. Melosh, G. H. Fredrickson, B. F. Chmelka, G. D. Stucky, *Science* **1998**, *279*, 548.
- [6] D. Zhao, Q. Huo, J. Feng, B. F. Chmelka, G. D. Stucky, *J. Am. Chem. Soc.* **1998**, *120*, 6024.
- [7] D. Zhao, P. Yang, N. Melosh, J. Feng, B. F. Chmelka, G. D. Stucky, *Adv. Mater.* **1998**, *10*, 1380.
- [8] P. Yang, D. Zhao, D. I. Margolese, B. F. Chmelka, G. D. Stucky, *Nature* **1998**, *396*, 152.
- [9] P. Yang, T. Deng, D. Zhao, P. Feng, D. Pine, B. F. Chmelka, G. M. Whitesides, G. D. Stucky, *Nature* **1998**, *282*, 2244.
- [10] R. Ulrich, A. Du Chesne, M. Templin, U. Wiesner, *Adv. Mater.* **1999**, *11*, 141.
- [11] S. M. De Paul, J. W. Zwanziger, R. Ulrich, U. Wiesner, H. W. Spiess, *J. Am. Chem. Soc.* **1999**, *121*, 5727.
- [12] I. W. Hamley, *The Physics of Block Copolymers*, Oxford University Press, Oxford, **1998**.
- [13] V. H.-Z. Chan, J. Hoffman, V. Y. Lee, H. Iatrou, A. Avegeropoulos, N. Hadjichristidis, R. D. Miller, E. L. Thomas, *Science* **1999**, *286*, 1716.

- [14] D. A. Huse, S. Leibler, *J. Phys.* **1988**, *49*, 605.  
 [15] J. Allgaier, A. Poppe, L. Willner, D. Richter, *Macromolecules* **1997**, *30*, 1582.  
 [16] A. C. Finnefrock, G. E. S. Toombes, S. M. Gruner, R. Ulrich, U. Wiesner, unpublished results.  
 [17] S. Brunauer, L. S. Deming, W. S. Deming, E. Teller, *J. Am. Chem. Soc.* **1940**, *62*, 1723.  
 [18] E. P. Barrett, L. G. Joyner, P. P. Halenda, *J. Am. Chem. Soc.* **1951**, *73*, 373.  
 [19] S. J. Gregg, K. S. W. Sing, *Adsorption, Surface and Porosity*, 2nd ed., Academic Press, **1982**.  
 [20] J. M. Thomas, *Angew. Chem.* **1999**, *111*, 3800–3843; *Angew. Chem. Int. Ed.* **1999**, *38*, 3588–3628.  
 [21] P. Ström, D. M. Anderson, *Langmuir* **1992**, *8*, 691.  
 [22] M. W. Tate, S. M. Gruner, E. F. Eikenberry, *Rev. Sci. Instrum.* **1997**, *68*, 47.

## Solvent-Free, Low-Temperature, Selective Hydrogenation of Polyenes using a Bimetallic Nanoparticle Ru–Sn Catalyst\*\*

Sophie Hermans, Robert Raja, John M. Thomas,\*  
 Brian F. G. Johnson,\* Gopinathan Sankar, and  
 David Gleeson

Progress in making solvent-free chemical conversions much more feasible than they are at present awaits the development of highly active (and selective) heterogeneous catalysts. Not only must the sites at which turnover occurs be of high intrinsic activity, their concentration (per unit mass) must also be large. Moreover, diffusion of reactant species to, and of products away from, such sites must also be facile.<sup>[1]</sup>

Herein we demonstrate how freely accessible active sites on bimetallic nanoparticles, finely dispersed and firmly anchored along the interior surfaces of high area (around 800 m<sup>2</sup> g<sup>-1</sup>) mesoporous silica function as highly effective catalysts for a number of selective hydrogenations that are of considerable significance for chemical and fine-chemical production. Such heterogeneous nanocatalysts may be readily prepared<sup>[2–5]</sup> from mixed-metal carbonylates and introduced in a spatially uniform fashion along the pores (around 30 Å diameter) of

the silica host. Their atomic structure is straightforwardly established,<sup>[1, 6–8]</sup> from in situ X-ray absorption and FTIR measurements.

Tin has been widely used as a “promoter” in heterogeneous catalysis, and has been shown to increase dramatically the selectivity of ruthenium catalysts in a variety of chemical transformations. These usually involve the selective hydrogenation of a carbonyl group in the vicinity of a conjugated or isolated double bond, such as the hydrogenation of benzoic acid and fatty esters to their corresponding alcohols<sup>[9, 10]</sup> or the hydrogenation of acrolein and its derivatives.<sup>[11]</sup> It has been suggested that the effect of tin is, besides others, to deactivate selectively certain catalytic sites on the surface thereby impeding undesirable side reactions.<sup>[10, 12]</sup> Other explanations, such as alloying and its consequential electronic influences, have also been proposed.<sup>[11]</sup>

The chemical conversions upon which we focus herein consist of the hydrogenation of cyclic polyenes: 1,5,9-cyclododecatriene, 1,5-cyclooctadiene, and 2,5-norbornadiene. The monoenes of all three polyenes are used extensively as intermediates in the synthesis of bicarboxylic aliphatic acids, ketones, cyclic alcohols, lactones, and other intermediates. The selective hydrogenation of 1,5,9-cyclododecatriene to cyclododecane and cyclododecene is industrially important in the synthesis of valuable organic and polymer intermediates, such as 12-lauro lactam and dodecanedioic acid,<sup>[13]</sup> which are important monomers for nylon 12, nylon 612, copolyamides, polyesters, and coating applications.

A wide variety of homogeneous and heterogeneous hydrogenation catalysts such as Raney nickel,<sup>[14]</sup> palladium,<sup>[15]</sup> platinum,<sup>[16]</sup> cobalt,<sup>[17]</sup> and mixed transition-metal complexes have been previously used for the above-mentioned hydrogenations.<sup>[18, 19]</sup> But all the reactions entailed the use of organic solvents (such as *n*-heptane, benzonitrile, and so forth),<sup>[13, 20–22]</sup> and some required utilization of efficient hydrogen donors such as 9,10-dihydroanthracene, often at temperatures in excess of 300 °C, to achieve the desired selectivities.<sup>[23]</sup> Recently, Reetz et al.<sup>[24]</sup> have shown that entrapment of palladium clusters in micro/mesoporous hydrophobic sol–gel matrices prevents undesired agglomeration of the clusters, to result in active catalysts for the hydrogenation of 1,5-cyclooctadiene.

Previously, we have described the catalytic performance of other, finely dispersed bimetallic catalysts (Ag–Ru,<sup>[2]</sup> Cu–Ru,<sup>[3]</sup> and Pd–Ru,<sup>[4]</sup>), some of which possessed remarkable properties. Herein we report the catalytic performance of a supported carbidic Ru<sub>6</sub>Sn nanoparticle and compare it with that of the above-mentioned bimetallic nanocatalysts. In particular, we highlight the changing selectivity (in the hydrogenation of 1,5,9-cyclododecatriene and other polyenes) as a function of operating temperature and degree of conversion.

The compound (PPN)[Ru<sub>6</sub>C(CO)<sub>16</sub>SnCl<sub>3</sub>] (PPN: bis(triphenylphosphane)iminium cation) is obtained in a two step reaction from the known carbido–hexaruthenium cluster [Ru<sub>6</sub>C(CO)<sub>17</sub>]. Details of the preparation along with the single-crystal X-ray structure of the anion [Ru<sub>6</sub>C(CO)<sub>16</sub>SnCl<sub>3</sub>]<sup>-</sup> (**1**), have been given elsewhere,<sup>[25]</sup> as have the corresponding details for the neutral species

[\*] Prof. Sir J. M. Thomas, Dr. G. Sankar, Dr. D. Gleeson  
 The Royal Institution of Great Britain  
 Davy Faraday Research Laboratory  
 21 Albemarle Street, London W1X 4BS (UK)  
 Fax: (+44) 0207-670-2988  
 E-mail: dawn@ri.ac.uk

Prof. B. F. G. Johnson, S. Hermans, Dr. R. Raja  
 Department of Chemistry  
 University of Cambridge  
 Lensfield Road, Cambridge CB2 1EW (UK)  
 Fax: (+44) 1223-339016  
 E-mail: jpt25@cam.ac.uk

[\*\*] We thank Dr. R. G. Bell for assistance with the computer graphics, Drs. P. A. Midgeley, V. Keast, and M. Weyland for help with STEM, and gratefully acknowledge the support (via a rolling grant to J.M.T. and an award to B.F.G.J.) of EPSRC and the award of a research fellowship (for G.S.) from the Leverhulme Foundation and a Marie Curie Fellowship within the TMR Programme of the European Commission (for S.H.).